Master's Thesis of Science Education

A Study on Antarctic Subglacial Lake using Cryosat-2 Satellite Radar Altimeter

Cryosat-2 위성 고도계를 이용한 남극 빙저호 연구

February 2016

Graduate School of Science Education
Seoul National University
Earth Science Major

Byeong-Hoon Kim

A Study on Antarctic Subglacial Lake using Cryosat-2 Satellite Radar Altimeter

Cryosat-2 위성 고도계를 이용한 남극 빙저호 연구

지도교수 서 기 원

이 논문을 교육학석사 학위논문으로 제출함

2015 년 12 월

서울대학교 대학원

과학교육과

김 병 훈

김 병 훈의 교육학석사 학위논문을 인준함

2016 년 1 월

위 원 장 _____

부위원장 _____

위 원 _____

Abstract

The ice surface measurements from satellite altimeter have discovered numbers of subglacial lakes since the surface height above active subglacial lake varies in accordance with the water storage of lake beneath ice sheet. In this study, the Antarctic subglacial lakes are studied by the Cryosat-2 satellite radar altimeter, which is the most recently launched by European Space Agency. The high-resolution processing of SARin mode yielding the elevation change rate ($=\Delta h/\Delta t$) enables us to verify the specific 2-D boundary of lake and to detect even the small-scale unknown lakes. In particular, the regions called 'Kamb Ice Stream' and 'Whillans Ice Stream' are the main study region of this thesis. In these regions the three subglacial lakes are newly discovered and those are named as Kamb Trunk 1, Kamb Trunk 2 and Upper Engelhardt, respectively. Those findings allow us to verify many of the previously unknown subglacial environments of corresponding area. First, the fluctuations of water storage in the lake Kamb Trunk 1 and Kamb Trunk 2 can be used to estimate the flow type of subglacial water on the ice-bedrock interface. Second, near the grounding line of Kamb Ice Stream, it is also discovered a downward vertical displacement in triangle-shaped region. Since the occurrence time of this event is coincident with the activities of upstream subglacial lakes, it could be a good example how the supply of subglacial water could affect the downstream ice thickness variation. Lastly, the discovery of Upper

Engelhardt subglacial lake is also very important clues to reveal the subglacial water pathway around Whillans and Kamb Ice Stream. The flow path revealed from the behaviors of subglacial lakes is coincident well with the simulation results that have been presented in several recent studies.

Keywords: Subglacial Lake, Cryosat-2, Satellite Radar Altimeter, Antarctica

Student Number: 2014-20974

Contents

Abstract **i**

Chapter 1 Introduction **1**

Chapter 2 Background **5**

2.1 Subglacial Lake in Antarctica 5

2.2 Hydrologic Background of Kamb Ice Stream 6

Chapter 3 Data and Method **9**

3.1 Cryosat-2 9

3.2 Cryosat-2 Data Post-processing 9

3.3 Hydraulic Potential and Streamline 11

Chapter 4 Result and Interpretation **13**

4.1 Subglacial Lakes around Whillans Ice Stream 13

4.2 Subglacial Lakes around David Glacier 14

4.3 Subglacial Lakes around Kamb Ice Stream 17

Chapter 5 Hydrologic Environment under the Trunk of Kamb Ice Stream **22**

5.1 Lake Boundary Decision 22

5.2 Hydraulic Flow Characteristics underneath the Kamb Trunk Lakes 22

5.3 Elevation Changes in the Kamb Trunk Esturary 29

Chapter 6 Discussion **35**

Chapter 7 Conclusion **39**

국문초록 **47**

List of Figures

Figure 1.1 Overview of our study region: Whillans Ice Stream, Kamb Ice Stream and David Glacier 4

Figure 2.1 The thermal condition beneath ice sheet that producing subglacial melt water 7

Figure 3.1 The hydraulic potential and its uncertainty around David subglacial lakes 12

Figure 4.1 The elevation change rate around Whillans & Mercer Ice Stream 16

Figure 4.2 The elevation change rate around David Glacier, the uncertainty map and the backscattering point cloud of Cryosat-2 measurement 18

Figure 4.3 The elevation change rate around Kamb Ice Stream 21

Figure 5.1 Ice surface elevations and its changes around the Kamb Trunk subglacial lakes 23

Figure 5.2 ICESat elevation measurements on Kamb Trunk subglacial lakes 24

Figure 5.3 Temporal volume change of subglacial lakes derived from Cryosat-2 elevation measurements within the lake area of Kamb Trunks 28

Figure 5.4 Elevation change in the estuary area near the grounding line of Kamb Trunk 3 32
Figure 5.5 Landsat images of the feature like a channel near the grounding line downstream of Kamb Trunk 3 33

Figure 6.1 Volume changes in the lakes upstream of KIS and the lakes in WIS 36

Chapter 1. Introduction

The surface elevation above polar ice sheet is usually governed by Surface Mass Balance (SMB), which involves snow accumulation, surface melting, wind drift and etc. A firn densification process [*Ligtenberg et al.*, 2011] and a dynamic effect like as change of ice stream velocity also can vary the ice thickness, thus it affects the surface elevation change. However, an active subglacial lake (SGL) also can causes a local change of surface elevation, because it triggers the transition of hydrostatic equilibrium according to the variation of its water level [*Siegert*, 2005]. In general, the surface elevation change forced by SGL's volume change is known as having smaller spatial scale than other factors. Furthermore, SGL have unusual cycle of drainage / filling event and moreover can alter the surface elevation from several tens of centimeters to several tens of meters. Therefore, it clearly could be distinguished from other factors by observing surface elevation change.

During last three decades, satellite altimeters have investigated a number of phenomena that are caused by changes in ice motion, by measuring the ice surface elevation in Antarctica. Especially with the spatial advantage of remote sensing, compared with ground based measurement, it is one of the most remarkable achievement that altimeters measured various unrevealed SGLs below the thick (tens to a few thousand meters) Antarctic ice sheet. *Siegert and Ridley* [1998] firstly discovered SGLs

below Antarctic ice sheet using satellite radar altimetry by taking advantage of the fact that the SGL can bring the ice surface to flatten. Subsequently, the laser satellite altimetry, ICESat launched in 2003, have measured the changes of surface elevation in high latitude regions, using on-boarded narrow and high frequency (laser) beams. *Smith et al.* [2009] observed several active SGLs in the Antarctica using a number of ICESat campaigns. However, the ICESat has limited spatial and temporal resolutions because it can measure the elevation change only along narrow and line-shaped backscatter points. Thus, it was not appropriate to sense the specific 2D ice surface boundary having elevation change of each SGL [*Siegert et al.*, 2014]. The paradigm of altimetry for land ice was recently shifted toward the Cyrosat-2 altimetry. Although its vertical resolution is lower than that of ICESat, the meandering footprint of Cryosat-2 has an ability to reaveal the 2-dimmentional structures of active SGLs in detail [*McMillan et al.*, 2013; *Siegfried et al.*, 2014]. The hydrological interaction between each of SGL has also been actively studied. *Fricker and Scambos* [2009] successively observed the hydrological connection between several SGLs in Whillans and Mercer Ice Stream (WIS & MIS), by measuring both of ice surface elevation and reflectivity changes from ICESat altimeter and MODIS images respectively. However, the ICESat could not measure small scale lake volume change by itself, and moreover MODIS image comparison on past works also have a limit that it can tell only a significant topographic change of given terrain which is induced by drastic drainage or flood event [*Flament et al.*, 2014; *Siegfried et al.*, 2014]. Meanwhile, studies for examining hydrological phenomena of

SGL using Cryosat-2 is still very scarce, even though its ability is enough to demonstrate these phenomena [*Flament et al.*, 2014; *Siegfried et al.*, 2014]. In this study, using the Cryosat-2 elevation measurements, the topographic change of the previously known subglacial lakes such as WIS and David Glacier are examined in order to test the accuracy of a detection method. The method is discussed in detail in Chapter 3.3. Data and Method. Sebsequently, the newly discovered SGLs, KT2 and KT3, which are located on the downstream of Kamb Ice Stream (KIS) are presented. Figure 1.1 displays the general information about these study regions. Ones can obtain physical environments for the regions such as their locations, morphologies, ice flow velocities and a location of previously known SGLs.

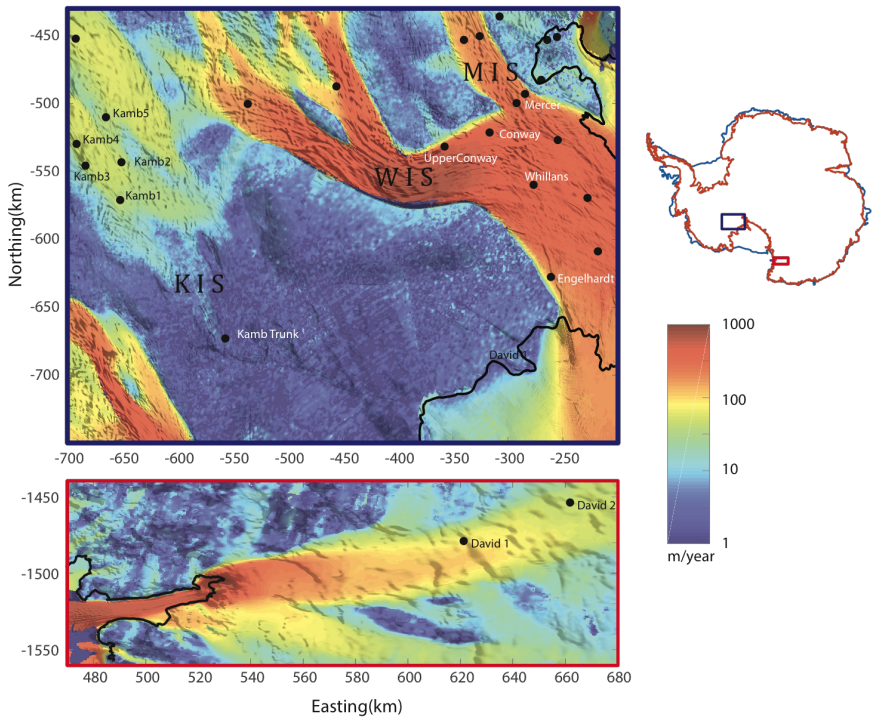

Figure 1.1. Overview of our study region: WIS, KIS (upper panel) and David Glacier (lower panel). The black dots are the subglacial lakes already categorized in the fourth inventory of Antarctic subglacial lakes [*Wright and Siegert*, 2012]. The main subglacial lakes are labeled. The color shading shows the InSAR-based ice velocity from MEaSUREs project [*Rignot et al.*, 2011], and background gray scale image reflects the surface morphology of each region from MODIS Mosaic of Antarctica (MOA 2009) image map [*Haran et al.*, 2014]. The black lines in both of panel are grounding line.

Chapter 2. Background

2.1 Subglacial Lake in Antarctica

There are many of lakes storing the liquid water underneath the Antarctic ice sheet. Those are generally called as 'subglacial lake', as mentioned at above Chapter. *Siegert* [2005] explains that this liquid water, subglacial melt water, is mainly generated by the three different causes. First, since the ice sheet is thick enough to form high-pressure environment on ice-bedrock interface, it can lower the melting point of bedrock-adjacent ice. Secondly, the ice sheet can produce the enough amount of liquid water in a region where the geothermal heat flux is higher than other regions (see Figure 2.1). Lastly, the frictional heat from fast flowing ice sheet also can make liquid water.

In the early 1970s, the existence of SGL has been revealed by in-situ explorations. *Robin et al.* [1970] firstly tried to measure the bedrock topography of Antarctic ice sheet using radio echo sounding (RES) profiles, and found out the existence of subglacial water. *Oswald and Robin* [1973] has explored the Lake Vostok, which is the largest subglacial lake in Antarctica, by using RES airborne surveys. Since the ice-water boundary has high reflectance in RES frequency (about 60 MHz), this method has been commonly used for detecting subglacial lake, even though it also has an ambiguity that cannot distinguish SGL from flattened region filled with the fine sediments [*Siegert*, 2005].

Satellite altimetry has also been utilized to locate SGL. At the first time, scientists deduce the locations of SGLs by the fact that the ice surfaces above SGLs have less inclination than other ice-covered region [*Siegert and Ridley*, 1998]. As the observation technique of ice surface elevation develops (i.e. the satellite imageries and the satellite altimeters), even the activity patterns of many SGLs were able to be identified accurately. *Wright and Siegert* [2012] presented the most recent integrated catalogue for 379 Antarctic SGLs, which includes active SGLs detected from airborne RES survey, RADARSAT In-SAR imagery, ICESat laser altimeter, and etc.

2.2 Hydrologic Background of Kamb Ice Stream

The KIS located on the boundary of eastern Ross Ice Shelf (Figure 1.1) has ceased its flow about a few hundred years ago [*Retzlaff and Bentley*, 1993]. It has been demonstrated that the cause of this stoppage was due to the abrupt sequential changes in the basal hydrological system [*Catania et al.*, 2006]. The stagnated state of KIS indicates the basal interface under the ice stream is mostly bonded to the bedrock below. Upper panel of Figure 1.1 shows that ice flow velocity in KIS, and this is comparable to those in MIS and WIS. Although the upstream of KIS where Kamb 1 – 12 lakes located still has an ice flow induced by basal sliding, the main trunk (downstream) of KIS has no sliding effect but has extremely little flow rate (about $5\,cm/yr$) which is probably caused by gravitational deformation of ice. Therefore, it would be possible to be channelized in downstream KIS if there were subglacial water flow.

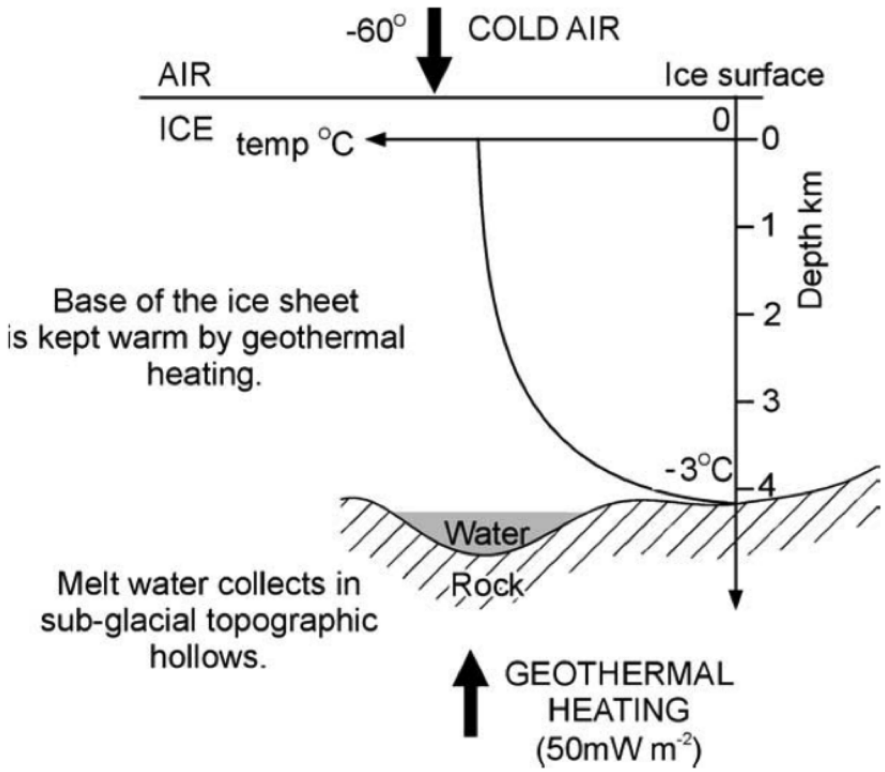

Figure 2.1. The thermal condition beneath ice sheet that producing subglacial melt water (from [*Siegert*, 2005]).

There are numbers of SGLs contributing the basal hydrology underneath the KIS (Figure 1.1). Although the existence of SGLs have been revealed by surface height variation from ICESat laser altimetry and RADARSAT radar interferometry [*Gray*, 2005], still little is known about the hydrological connection among adjacent lakes in KIS. Moreover, the ICESat repeat track method has a critical flaw that the superposed ground tracks are too sparse to determine the lake boundaries in details or to map small lakes entirely. At present, the northern corner of KIS is morphologically understood as a margin lake due to thinning along a shear margin or advance of grouding line, similar to the lake Engelhardt downstream adjacent to Whillans Ice Stream. *Goeller et al.* [2015] and *Fried et al.* [2014] suggests that a persistent subglacial channel still exists beneath KIS, based on the evidence of their own numerical models. However, the ICESat could not detect any signal due to subglacial lake activity in the margin of KIS trunk during its working period.

Chapter 3. Data and Method

3.1 Cryosat-2

The Cryosat-2 operates three different modes, Low Resolution Mode (LRM), Synthetic Aperture Radar (SAR), and SAR interferometric (SARin) [*Wingham et al.*, 2006]. The SARin mode has an advantage of determining the accurate reflecting (backscattering) point on the earth surface by the technical support of on-boarded dual antennas. A nominal spatial resolution of this mode measurement is $300m$ and $1km$ for along and across track directions, respectively [*Wingham et al.*, 2006]. The geophysical mask of SARin mode covers the margin of ice sheet or mountainous region, which usually have higher slope than the ocean or ice sheet interior. We primarily utilize the Level 2 (L2) product of SARin mode, which directly serves geophysically-corrected surface elevation with various correction terms and error flags. The accuracy of SARin mode ranges from $0.17m$ to $0.65m$ on the interior of ice, although the magnitude of surface height error highly depends on the slope of reflected surface [*Wang et al.*, 2015].

3.2 Cryosat-2 Data Post-processing

For the detection of marginal SGLs, a conventional method for measuring the linear trend of surface height over Antarctica using Cyrosat-2 [*McMillan et al.*, 2014; *Siegfried et al.*, 2014; *Wouters et al.*, 2015] is ap-

plied with slight modification. At first because Baseline B elevation data suffers from its instrumental bias [*McMillan et al.*, 2013], which is about $0.673m$, we add $0.673m$ to elevation values of Baseline B. Then we extract data around observing area and remove a data containing height error flag (which contain error in height derivation from waveform data) or having backscatter value over 30 (dB/100). For $5*5km$ grid space, we subtract topographic effect from a elevation model derived by Cryosat-2 [*Helm et al.*, 2014] and iteratively applied 3 sigma filter. In this way most of the measurement error and time-invariant components are removed effectively.

Then we fit the residual data by quadratic curved surface to eliminate the remaining topographic effect, because the remaining slope makes it difficult to calculate exact temporal height variation. After averaging the entire time-series for every month, two-year linear trends are estimated at a month interval. The model equation used here is as follows:

$$h(t) = a_0 + a_1 x + a_2 y + a_3 x^2 + a_4 y^2 + a_5 xy + a_6 t,$$

where h is surface elevation dataset, x and y are easting and northing value (unit : km) of polar stereographic coordinate, which is converted from longitude and latitude of each measurement point. t is measurement time and thus a_x are regression coefficients.

For example, the monthly averaged Cyrosat-2 data have 60 months (July 2010 June 2015) time-series for height variation, but the 'change rates ($\Delta h/\Delta t$)' derived from above functional fit have 37 (months) time series from July 2010 – June 2012 to July 2013 – June 2015 for each grid. This method effectively reduces noise and can detect periodic elevation

changes associated with activity of SGLs.

3.3 Hydraulic Potential and Streamline

The subglacial channel from BEDMAP2 data can be generated from the gradient of hydraulic potential (P_h) that is calculated as follows:

$$P_h = \rho_w g z_b + \rho_i g z_i,$$

where ρ_w and ρ_i are density of water (1000 kg/m^3) and ice (917 kg/m^3), z_b and z_i are bedrock elevation and ice thickness, respectively. According to *Fretwell et al.* [2013], bedrock topography of BEDMAP2 is derived from the difference between ice surface topography and ice thickness measurement from various observations. Thus the uncertainty of hydraulic potential is due to both of uncertainties. For example, the lower panel of Figure 3.1 shows the uncertainty of hydraulic potential (P_{h_unc}) and it is calculated as follows:

where z_{b_unc} and z_{i_unc} are the uncertainties of bedrock elevation and ice thickness respectively. When we consider the uncertainties of bedrock elevation and ice thickness are not correlated with each other, $z_{b\_unc*i\_unc}$, which is the covariance of them would be zero. Therefore, the uncertainty expression above could be simplified as follows:

$$P_{h\_unc} = (\rho_w^2 g^2 z_{b\_unc}^2 + \rho_i^2 g^2 z_{i\_unc}^2)^{1/2}.$$

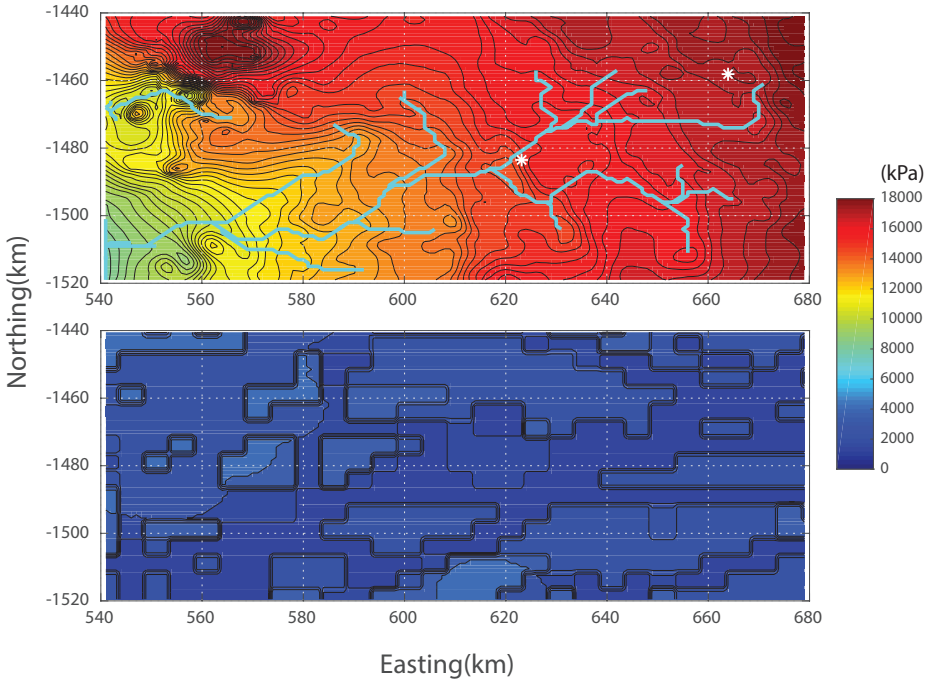

Figure 3.1. The hydraulic potential and its uncertainty around David SGLs.

Chapter 4. Result and Interpretation

4.1 Subglacial Lakes around Whillans Ice Stream

Figure 4.1 displays the surface elevation change rate around WIS. There are both regular and irregular changes due to lake activities and noisy signals. In the first stage (July 2010 – June 2012, top panel of Figure 4.1(a)), the positive change rates of Upper Conway and Conway SGLs are distinct. This indicates that these lake volumes increased in that period, which might be triggered by a water supply of upper stream, but other signals on the ice stream region are interpreted as noises because they show irregular spatial pattern and have large uncertainties.

In the second stage (Nov. 2011 – Oct. 2013, middle panel of Figure 4.1(a)), a drainage process was ongoing in the Upper Conway and Mercer. At the same time, the background elevation, i.e. the elevation in the region adjacent to the SGLs, is mostly increased in comparison with the previous stage. Since the WIS has been slowing down [*Joughin and Tulaczyk*, 2002], it is expected that the ice is thickening around this region. However, the ice thickness change rate of this region also varies during each of time span, because the ice stream velocity changed inter-annually due to subglacial hydrology [*Beem et al.*, 2014].

The drainage of Conway is remarkable in the third stage (Aug. 2012 – July 2014, upper panel of Figure 4.1(b)). However, there are also filling signals (positive change rate) on Whillans and Engelhardt, and a

drainage signal (negative change rate) at [-450km, -540km] in the polar stererographic coordinate during this period. We assume that the negative signal area is a newly discovered SGL, and preliminarily name it as 'UpperEngelhardt'. The existence of this lake could be supported by the modeled subglacial channel(cyan line) because it clearly penetrates the lake area we predict.

4.2 Subglacial Lakes around David Glacier

For David Glacier, it was not successful to apply the method introduced previous section because the ice surface of David Glacier is too rugged so that the backscattering points of Cryosat-2 beam are distributed quite heterogeneously. Thus, we need to calculate the $\Delta h/\Delta t$ with longer time series data than other region. Figure 5 shows the $\Delta h/\Delta t$ for the time span of July 2010 to Feb. 2015 on the David Glacier region. Despite the total change rate values are derived from better spatial coverage than 2-year change rate, in this figure irregular positive and negative signals are exhibited, and this spatial feature hinders locating active subglacial lakes. Thus the uncertainty map (the second panel) is useful to fix this limitation. Figure 4.2 shows that most regions of higher positive or negative change rate values also have higher uncertainties. The measurement (backscattering) point of satellite shown in the last panel may also be helpful in selecting the actual signals. In this figure, the white area indicates no measurement region, so the signals in those regions could be considered as regression error.

Among the elevation change signals shown in the top panel of Fig-

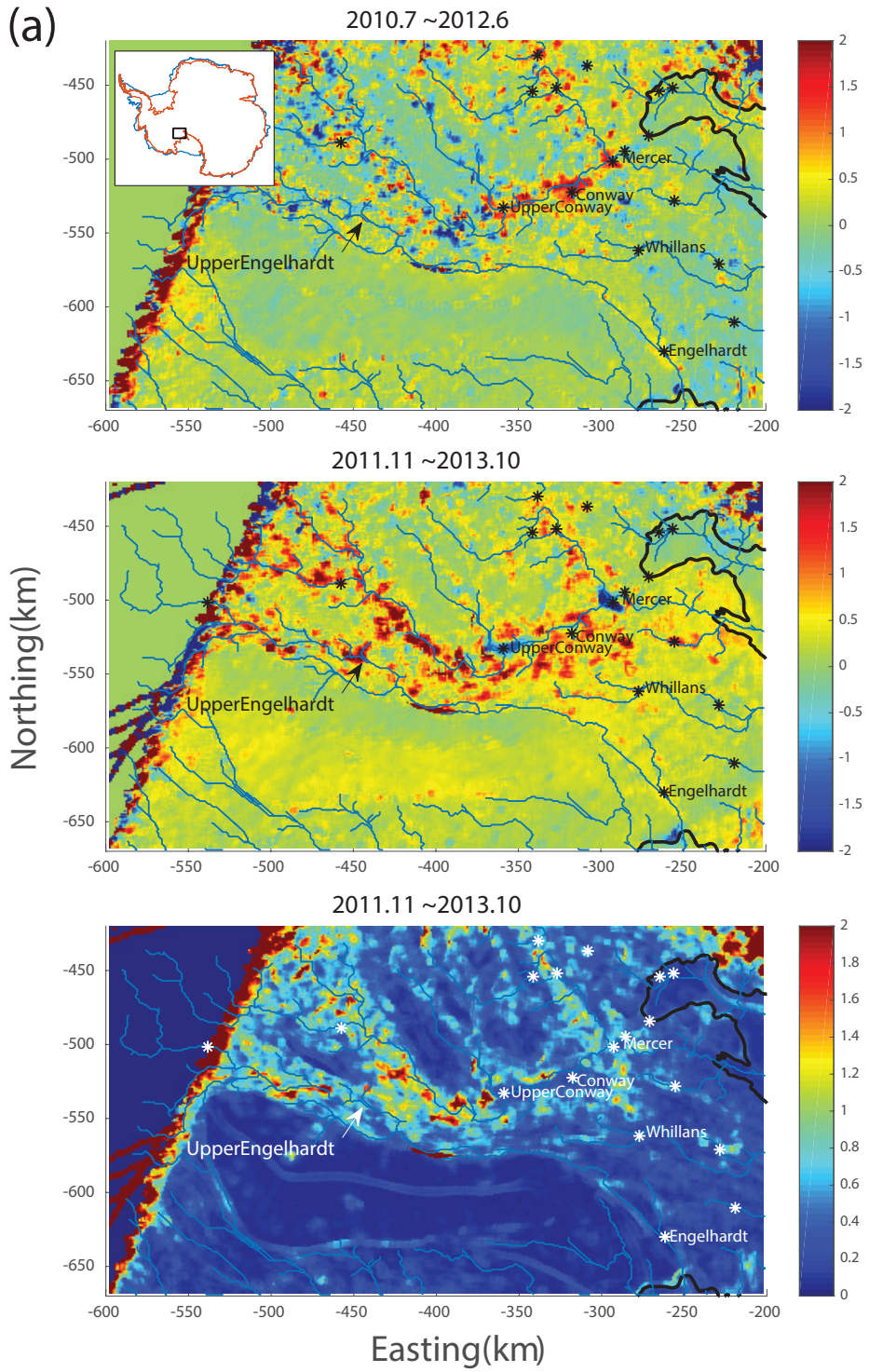

Figure 4.1. *(continued)*

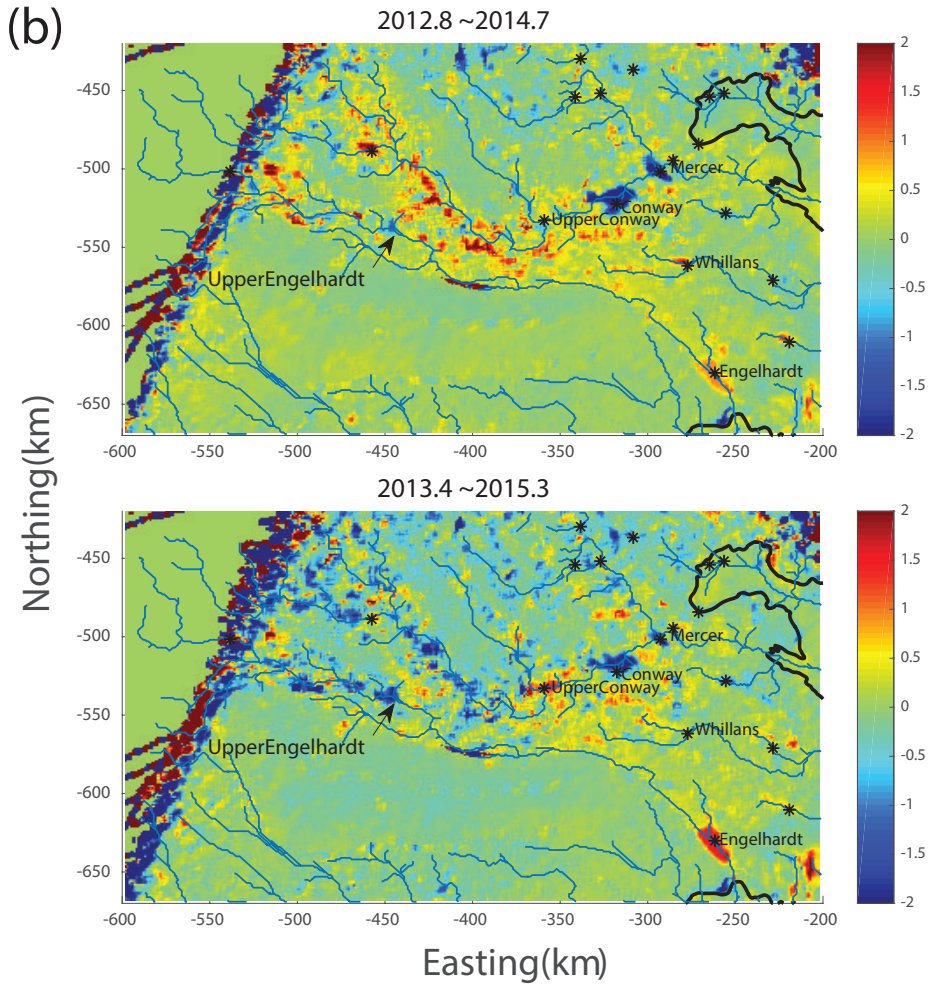

Figure 4.1. The elevation change rate ($\Delta h/\Delta t$, unit = m/yr) around Whillans & Mercer Ice Stream (Ice Stream B) on the polar-stereographic coordinate. Δt is commonly calculated as 24 months. The bottom panel of (a) is the uncertainty of change rate on second stage (middle panel of (a)) with 95 % confidence interval. Four $\Delta h/\Delta t$ figures are divided to two sections (a) and (b), due to the limitation of page area. The cyan solid line denotes the possible flow line estimated from BEDMAP2 ice thinkness bedrock topography data. The black star shows the location of subglacial lakes that were discovered by a previous study [*Smith et al.*, 2009; *Wright and Siegert*, 2012]. In this research, 'Upper Engelhardt' subglacial lake is discovered. The black solid line means grounding line. A white sub-panel in top panel of Figure (a) shows the location of given region.

ure 4.2, the two signals where arrows indicate might be induced by the water level variation of active SGLs, David 1 and David 2. The horizontal scales of those two lake areas are similar with those of measured from ICESat [*Smith et al.*, 2009]. However, it is also remarkable that the locations of those two lakes are slightly shifted from reported locations in the previous study. The location of David 1 is about $20km$ northwest away from reported region, and David 2 is also about $5km$ away in the same direction. Regarding to this mismatch of lake location, it is presumed that ICESat had mislocated the spatial coverage of those two SGLs, because it only measures the surface height variation via narrow beams and therefore it has less horizontal resolution than Cryosat-2. The two SGLs observed here are not located on the modeled flow line (cyan). This is probably because the BEDMAP2 have large uncertainties due to the scarcity of *in-situ* bedrock topography measurements (lower panel of Figure 3.1). Consequently, all of three evidences (ICESat, Cryosat-2, and predicted subglacial channel) for inferring SGL are ambiguous in current state. Further effort is needed to locate the SGLs in the David glacier using in-situ measurements such as airborne radar survey, seismic exploration, or GPS monitoring.

4.3 Subglacial Lakes around Kamb Ice Stream

The method used in the WIS region is applied in the trunk of KIS. Figure 4.3 clearly shows the surface elevation changes on the Kamb Trunk (KT1) lake, which is previously reported in ICESat observation [*Smith et al.*, 2009]. During the observation period, KT1 temporarily had a posi-

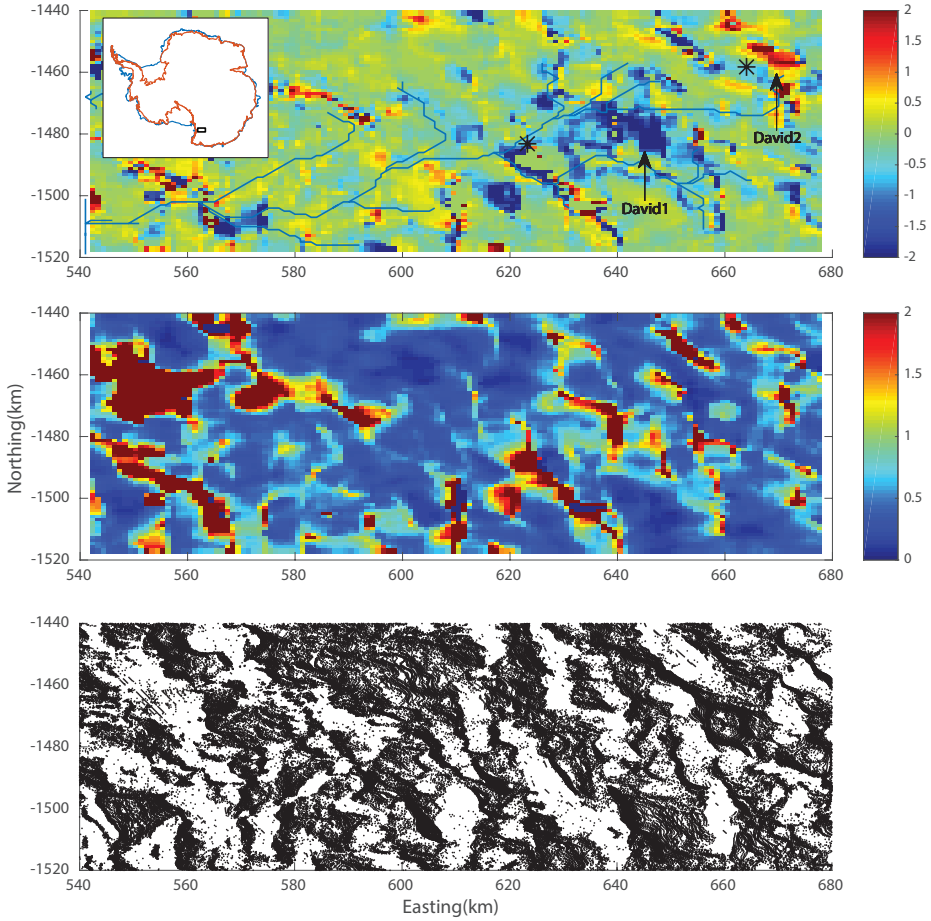

Figure 4.2. The elevation change rate ($\Delta h/\Delta t$, unit = m) around David Glacier (top panel) , the uncertainty map (middle panel) and the backscattering point cloud (bottom panel). Since the David Glacier has many of crevasses and rugged bedrock topography, the backscattering point (which is the most nearest point to satellite) could be focused on the higher terrain region. Thus, the lower terrain could have large uncertainty in the dh/dt calculation.

tive $\Delta h/\Delta t$ and soon disappeared, thus we assume that there was a filling event and it has not been drained until recent time. Interestingly, while the level of KT1 changes, it is also observed the surface elevation changes that were not reported before in the two areas of the downstream (indicated by arrows). The elevation change signals are thought to closely linked to the upstream KT1 because they are located along the flow line, and thus those are regarded as active SGLs that is newly discovered in this research. We name the lakes as Kamb Trunk 2 (KT2) and 3 (KT3), because they seem to be provoked by an upstream lake KT1. Figure 4.3 also shows that these three lakes in the trunk of KIS simultaneously experienced a sudden filling event in the middle of 2013.

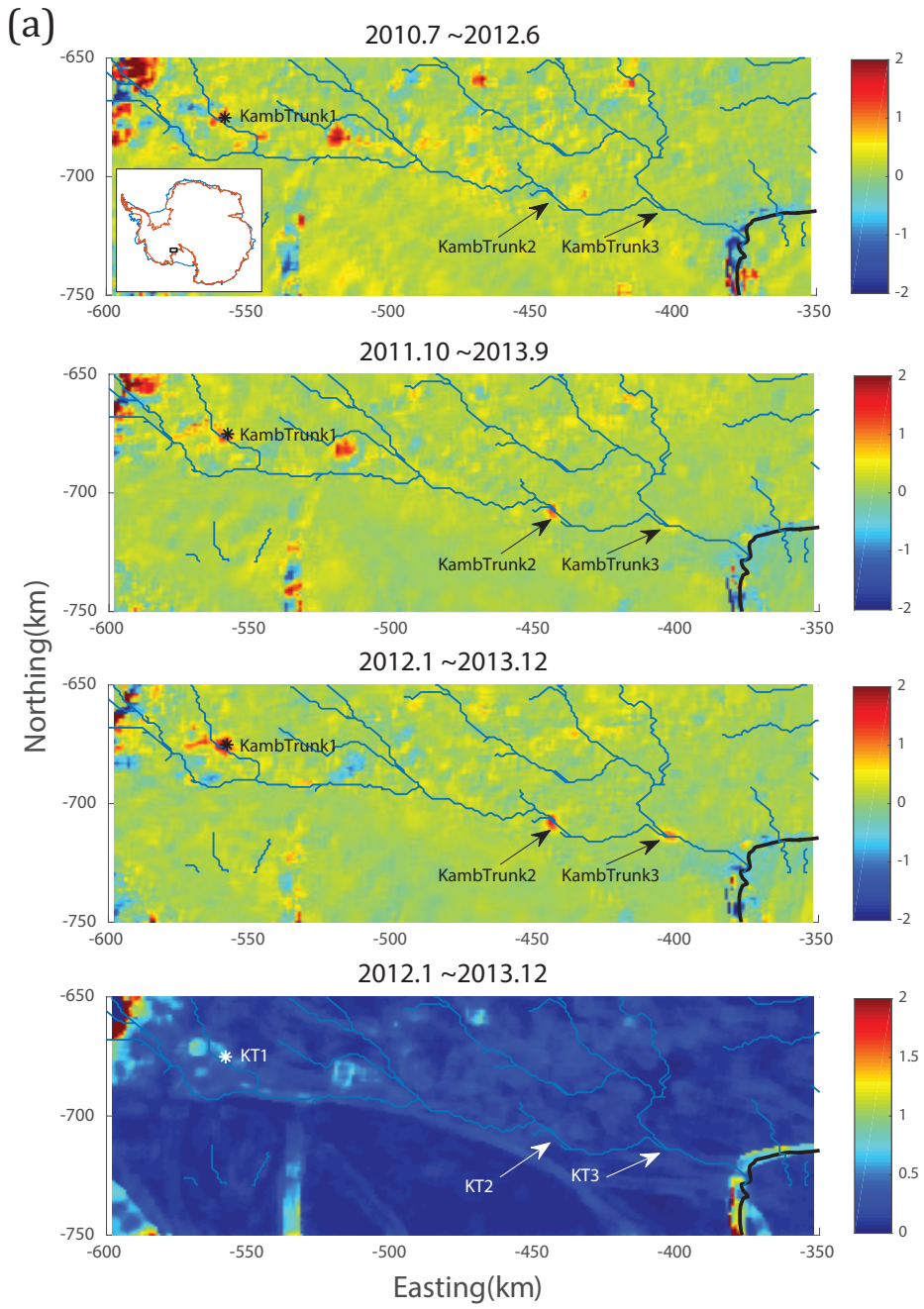

Figure 4.3. *(continued)*

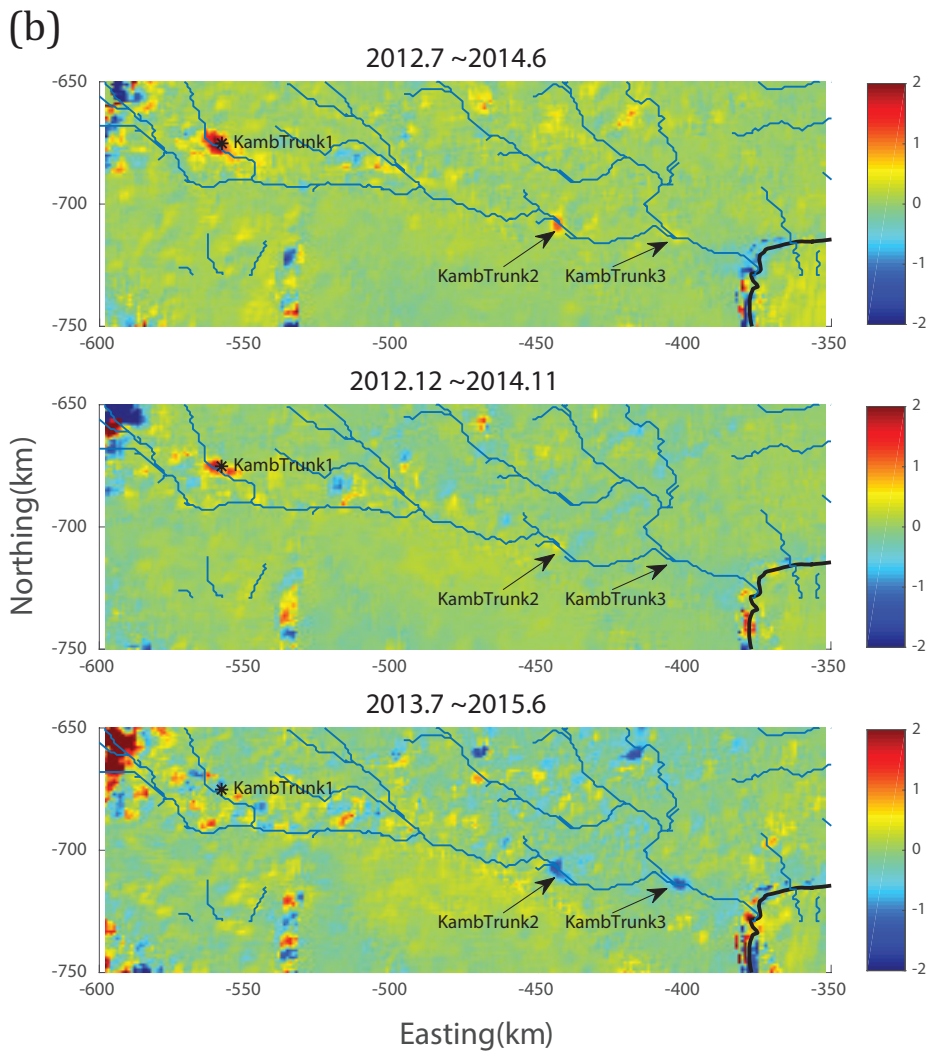

Figure 4.3. The elevation change rate ($\Delta h/\Delta t$, unit = m/yr) around Kamb Ice Stream. 'Kamb Trunk 2 & 3' subglacial lakes are discovered in this research. The explanation for this figures is same with Figure 3.

Chapter 5. Hydrologic Environment under the Trunk of Kamb Ice Stream

5.1 Lake Boundary Decision

In order to specify the boundary of the SGLs in the trunk of KIS (Figure 5.1), it is used that the difference between two digital elevation models (DEMs) in regularly spaced $200m$ grid, generated using Cryosat-2 elevations in two different time periods and the ordinary kriging with Gaussian semivariogram [*Goovaert*, 1997]. The two different time periods are selected as July 2010 – December 2011 before filling events and May 2013 – January 2014 after filling events except for KT1 (May 2013 – January 2015 after filling events for KT1). In the difference map of two DEMs, a contour line with a value same as the standard deviation of difference map is empirically chosen as the lake boundary, since such a choice of contour line makes a good agreement with the lake boundary shown in the repeat track analysis of ICESat measurements in the case of KT1 (Figure 5.2). Approximately, the area of KT1, KT2, and KT3 are 43.5, 31.7, and 38.7 km^2, respectively.

5.2 Hydraulic Flow Characteristics underneath the Kamb Trunk Lakes

Figure 5.3 displays the volume changes of three SGLs, estimated from the averaged Cryosat-2 elevation within the lake boundary and the area

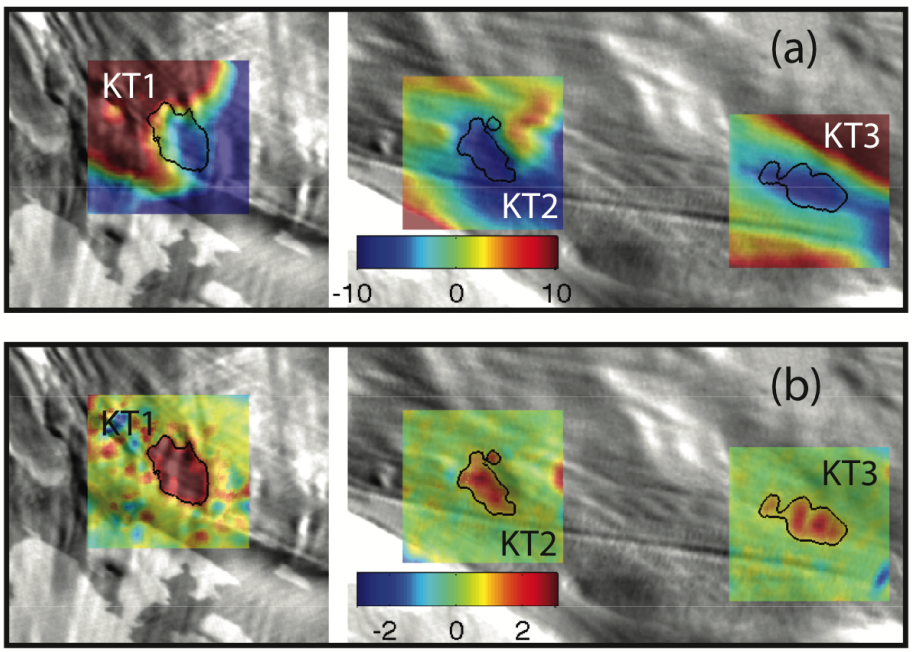

Figure 5.1. Ice surface elevations and its changes around the subglacial lakes. (a) Reference surface topography (color shading) derived from the Cryosat-2 elevation measurements in the period from Jul. 2010 to Dec. 2011. Note that the mean elevation values in each rectangular area were subtracted in order to show the fine-variant elevation in detail. (b) Elevation anomalies with respect to the reference topography in the period from Jan. 2014 to Mar. 2015 for KT1 and from Jul. 2013 to Jan. 2014 for KT2 and KT3. The elevation unit in (a) and (b) is m and the background is the MOA image.

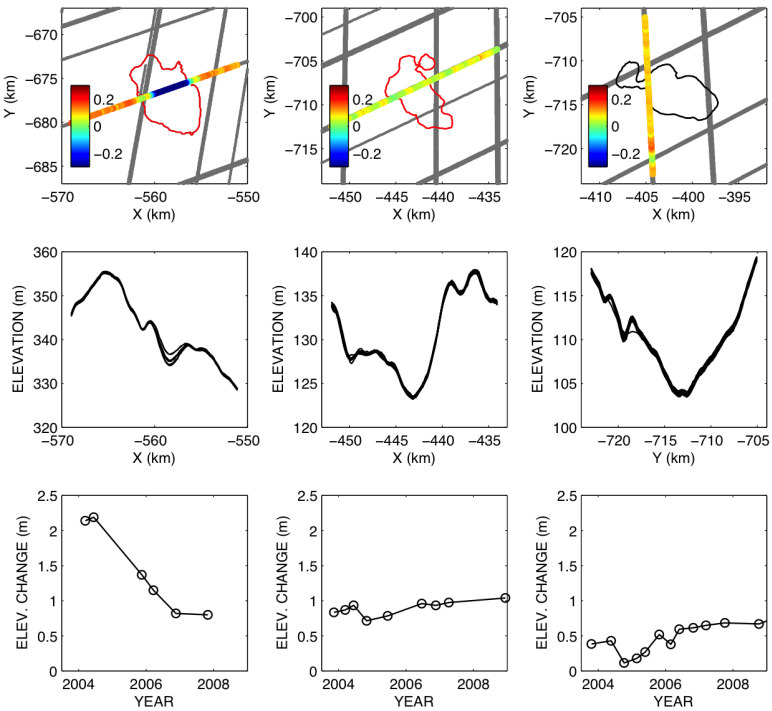

Figure 5.2. ICESat elevation measurements on KT1 (left column), KT2 (middle column) and KT3 (right column). The upper rows show the ICESat elevation change rates (m/yr) along the tracks crossing the lakes (color scatter). The middle and lower rows show the elevations along the tracks and the temporal elevation change in the lakes respectively.

of SGL. The background elevation changes outside of lake boundary are removed before the volume estimation. The volume changes clearly show a sequential filling event in 2013. If we assume the sequential time delay of elevation jumps are entirely due to the travel time of subglacial flow between the SGLs, the sequential filling event allows us to infer the flow velocity among the SGLs. In order to determine the start time of filling event from the coarse time series with large sampling intervals, we choose two points, indicated as circles in Figure 5.3, clearly identified as the beginning of filling in each time series and assume their midpoint as the start time of filling. The time delay is $\sim$ 2.9 months between KT1 and KT2 and $\sim$ 1.6 months between KT2 and KT3. Note that substantial uncertainties can be imposed in picking the start time of filling, due to the large sampling interval of volume change ($\sim$ 0.1 year) caused by the repeat interval of Cryosat-2 passing through the SGLs. In order to calculate the flow distance, the flow line between the SGLs is extracted from the hydraulic potential surface [*Schwanghart and Kuhn*, 2010] (e.g. cyan line of Figure 6). The flow distances between KT1 and KT2 and between KT2 and KT3 are $\sim$ 147 km and $\sim$ 50 km respectively. If we assume the time uncertainties of two points as the half of mean time interval ($\sim$ 0.05 year) and the uncertainties of the flow distance along the inferred subglacial flow line as 10 %, the subglacial flow velocities are estimated as 69 ± 16 and 44 ± 17 m/hr, respectively.

In situ measurements of basal water flow speed have been gathered by many glaciological investigations. For instance, tracer tests have revealed the water flow speeds beneath several glaciers in the northern hemisphere,

i.e. 72 m/hr in the basal system of Variegated Glacier, Alaska [*Kamb et al.*, 1985], 40–432 m/hr in South Cascade Glacier [*Fountain*, 1992], 41 m/hr in Trapridge Glacier [*Stone and Clarke*, 1996]. In the Antarctica, a direct measurement of subglcial water velocity was made on Whillans Ice Stream giving 27 m/hr in average [*Engelhardt and Kamb*, 1997]. Considering these in situ measurements, the velocities inferred from the sequential delay of lake filling event in the trunk of KIS are reasonable values as basal water flow velocities.

The estimated water velocities provide another information about subglacial hydraulic conditions. In various ice sheet models as reviewed by *Flowers* [2015], the subglacial water velocity v can be written as

$$v = \frac{1}{n} R^p \Big[\frac{\nabla \phi}{\rho_i g} \Big]^q \tag{5.1}$$

with Manning roughness n, hydraulic radius R, hydraulic potential ϕ, density of ice ρ_i, and gravitational acceleration g. The values of exponents are theoretically p=2, q=1 for laminar and p=1/2, q=1/2 for turbulent flow. If we assume the subglacial environments between KT1 and KT3 are homogeneous i.e. the parameters except for hydraulic potential are constant, the water velocity is linearly dependent to $[\nabla \phi]^q$. In this assumption, the substitution of the water velocities and hydraulic potential gradients estimated along the flow line among the three SGLs into equation (5.1) gives $q \approx 0.6 \pm 0.2$. Consequently, we can infer the subglacial water flow between KT1 and KT3 is analogous to turbulent flow and probably a channelized flow connects the SGLs.

The patterns of three lake's volume changes are a bit ironic. Despite they monotonously linked, their shapes are not identical each other. (Al-

though we cannot guess yet about further KT1's lowering pattern, it has been observed not drastic but gradual volume decrease in the past ICESat era (Figure 5.2)). Furthermore, if we are trying to explain this pattern to a simple circuit, which is governed by the uniform fluxes input and output, for example, there would be no way to explain the KT2 drastic drainage event in the middle of 2014, without any change of KT3 (Figure 5.3). It implies that the output flux of lake could drastically increase according to other factors.

One possible explanation is that each of three patterns of water level change is associated with different basal environments. The drastic level increase of each lake can be plausibly interpreted as the increase of input flux, due to the upstream sudden drainage event. The sequential stage is balanced flux, which is the input flux is nearly equal with (or slightly less than) output flux. The last stage, it is not certain but might be presumed as a burst of output flux. Since SGLs are placed under the high-pressure basal environment, an inflating or a deflating 'balloon-like' effect might be triggered depending on the condition of ice-bedrock interface, such as a sediment leakage in front of drainage channel. Indeed, *Fricker and Scambos* [2009] observed sequential drainage event of two-connected SGLs (Conway and Mercer) in Whillans & Mercer Ice Stream, and also their upper drainage — lower refilling event was not always coincident. This implies that a downstream SGL's water level could be undeterred by a magnitude of upstream water supply. However, this perspective is still conjectural, because the short periodic flow models for subglacial flooding activities are much scarcer than decadal (or more) scale models.

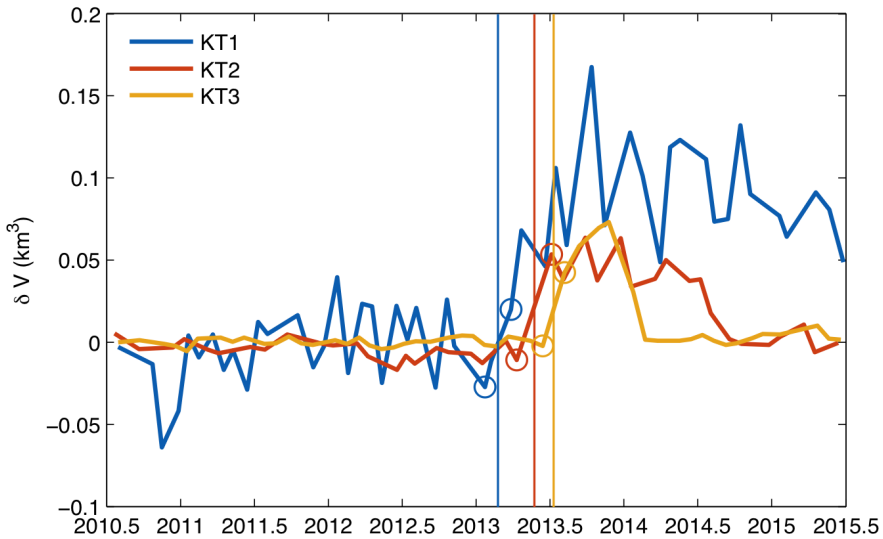

Figure 5.3. Temporal volume change of subglacial lakes derived from Cryosat-2 elevation measurements within the lake area defined in Figure 2.1. The vertical lines indicate the start times of filling events and the circles are the data points used for the determination of start time.

An historical research for connected SGLs and the result of this study would help to make a plausible mechanism for explanation of above lake activities.

5.3 Elevation Changes in the Kamb Trunk Estuary

The estuary downstream of KT3 has an elevation change corresponding to the lake activity in KT3 (Figure 5.4). By combining with ICESat data, we find that the estuary has three-stage variation. In ICESat era, the elevation decrease at a rate of $0.1m/yr$, but in the early of Cryosat-2 era the rate reduces by half. This is probably associated with the cessation of KT1 drainage event after 2007 (Figure 5.2). Since the early 2013, the surface elevation in the estuary region drastically decreases at the rate of $0.25m/yr$, indicating that the ice thickness in the estuary region is regulated by the upstream water supply. Then, why does the ice thickness decrease around the estuary? It is presumed that a part of basal water flow from KT3 is converted to laminar flows like water sheets and films in the estuary, since the hydraulic potential around the estuary has a shape like a fan (Figure 5.4(a)). If the distributed basal water increases the lubrication of ice sheet bed and decreases drag force of ice sheet flow, the tensile force inherent between moving ice shelf and stagnant grounded ice can stretch and thin the ice sheet. This hypothesis is supported by the fact that the ice sheet around the estuary is not entirely stagnant, i.e. ice flow velocity from InSAR [*Rignot et al.*, 2011] around estuary exceeds their uncertainty (Figure 1.1). The future work on a simultaneous tracking of

ice flow velocity and ice thickness in this area would be helpful to prove this hypothesis.

On the other hand, The MODIS MOA image shows a feature like narrow channel near the grounding line downstream of KT3 (Figure 5.4(a)). Though the feature is too concave for the Cryosat-2 to measure its inside elevations, we can clearly observe a strong thinning of ice ($\sim$1 m/yr) inside the feature through the ICESat elevations (see the inset in Figure 5.4(d)). We suppose that this feature was formed by a basal melting induced by the outflow of subglacial water into the sub-ice-shelf cavity. *Le Brocq et al.* [2013] proposed a plausible physical mechanism to explain a line-shaped cave pattern on the ice shelf surface. They showed when the subglacial melt water in grounded ice sheet flows to oceans, heat can be supplied from warmer ocean water to ice, thus floating fresh water could dissolve the lower part of ice shelf. If this mechanism is applied to the KIS, the strong basal melting by the outflow of subglacial water can make a narrow cavity beneath grounding line extending toward upstream, since the KIS ceased its ice flow $\sim$150 years ago. Indeed, glancing at the Landsat images in 1999 and 2014, we can find the feature is extending toward upstream (Figure 5.5). Considering the retreat rate of the feature ($\sim$70 m/yr), the retreat seems to begin after the stagnation of KIS. Consequently, it is speculated the feature results from a subglacial melt water channel linked to sub-ice-shelf cavity and this speculation is another evidence for the existence of a channelized water flow from KT1 to grounding line.

Since the similar feature is not observed around the margin of KIS, it

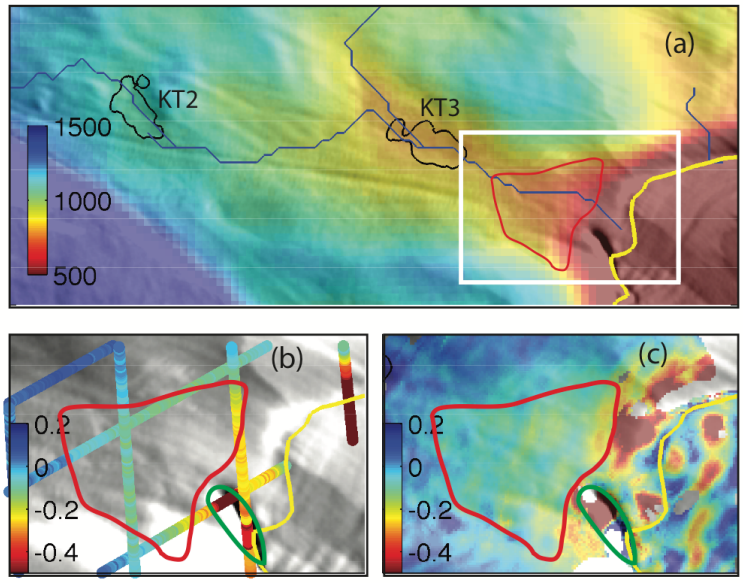

Figure 5.4. *(continued)*

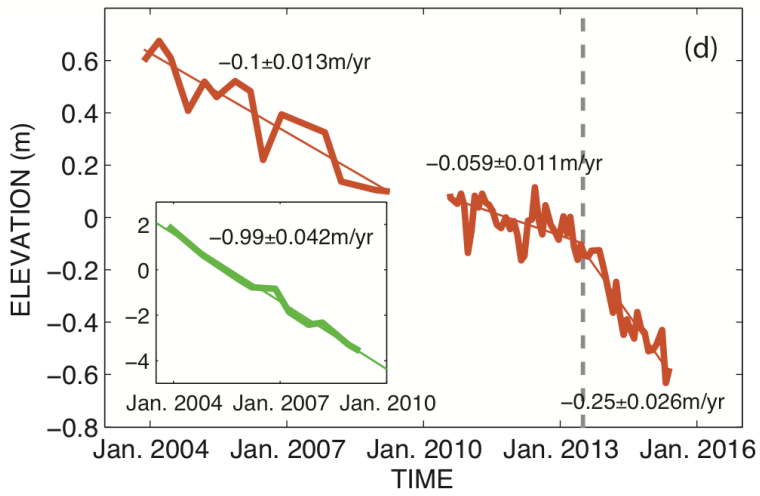

Figure 5.4. Elevation change in the estuary area near the grounding line (yellow line). (a) Hydraulic potential (color shading) and flow lines (blue line). The unit of hydraulic potential is kPa. The white retangle indicates the area displayed in (b) and (c). (b) Elevation change rate estimated from ICESat repeat track analysis. (c) Elevation change rate calculated from the Cryosat-2 elevation difference between 2010 – 2011 and 2014 - 2015. (d) Temporal elevation changes of ICESat and Cryosat-2 measurments in the red polygon in (b) and (c). The bias between ICESat and Crysat-2 elevations including the instrument bias ($0.67m$) and the effect of radar penetration into the snow pack ($1.03m$) which is estimated along an adjacent ICESat track was removed from the ICESat elevation. The gray dashed line indicates the filling event of KT3 lake. The inset shows the ICESat temporal elevation change in the feature like a channel (green polygon) near the grounding line.

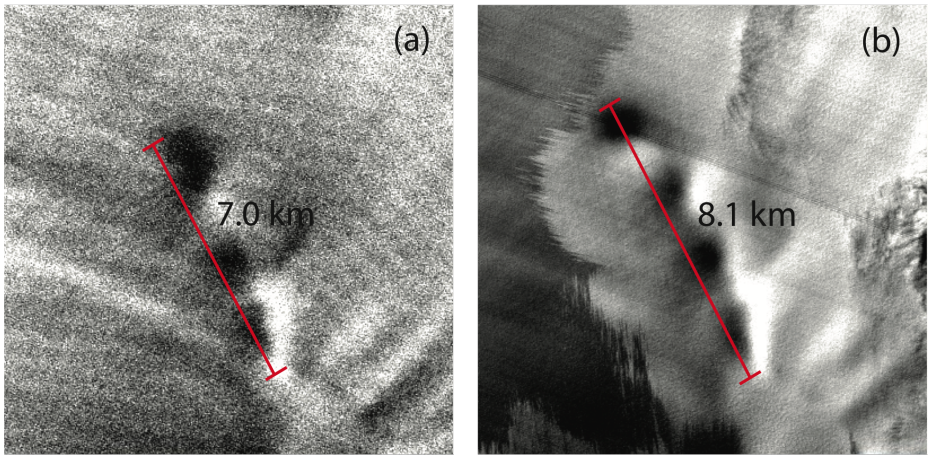

Figure 5.5. Landsat images of the feature like a channel near the grounding line downstream of KT3 in (a) 1999 and (b) 2014.

is considered that the KIS downstream only have single subglacial channel which reaches grounding line, as predicted by previous model results [*Carter and Fricker*, 2012; *Goeller et al.*, 2015]. The basal water tributary derived by hydraulic potential (Figure 5.4(a)) also supports this contention. On the other hand, Cyrosat-2 could not observed elevation change in this area because it measures elevation in closest reflecting point so that is not proper for such plunging area.

Furthermore, at least the past dozens of years, it is considered that the sub glacial water existed incessantly through this single channel, which penetrates KT1–3 SGLs. First, the elevation of KT estuary decreases even before KT1 lake activity at the rate of $0.1m/yr$. Moreover, the flow patterns of KT1–3 imply that the activity of downstream SGL is not connected to upstream activity. This indicates that this single subglacial channel always has small amount of water flow, or the ice and bedrock interface is wet enough to reduce the drag force of ice stream.

Chapter 6. Discussion

To investigate causes of the hydrological change that occurred nearby the trunk of KIS, we should pay attention to the upstream source of reservoir. However, in the upstream region, the geographical mask of Cryosat-2 SARin mode does not cover in this area so that the surface elevation can be measured by only LRM mode, which have relatively much poorer spatial resolution than SARin mode. Thus, in the case of the subglacial lake located on the upstream of KIS, we can roughly measure just an elevation change of SGL with our method. The upper panel of Figure 6.1 denotes the elevation change of the lake K1, K34, and K8, which located on the upstream of KT lakes, measured from the LRM mode of Cryosat-2. The lake K34, which is a large lake probably misidentified as two lakes K3 and K4 in *Smith et al.* [2009], was filled up to its maximum capacity in early 2012 and then start to drain and fill water into the lake K1 downstream of K34. The water drained from K34 increased the volume of lake K1 for up to 0.3 km^3. The lake K1 also started to drain in early 2013. After the drainage of K1, the lake KTs located at downstream of K1 experienced sequential filling events. Based on the gradient of hydrological potential, the drainage from lake K1 is believed as a source of the sequential filling events in the lake KTs. The lake K8 located at upstream of K1 drained the water of 0.1 km^3 in the end of 2012. The drainage of K8 may also be a source of the filling in lake KTs and the lakes in WIS partly.

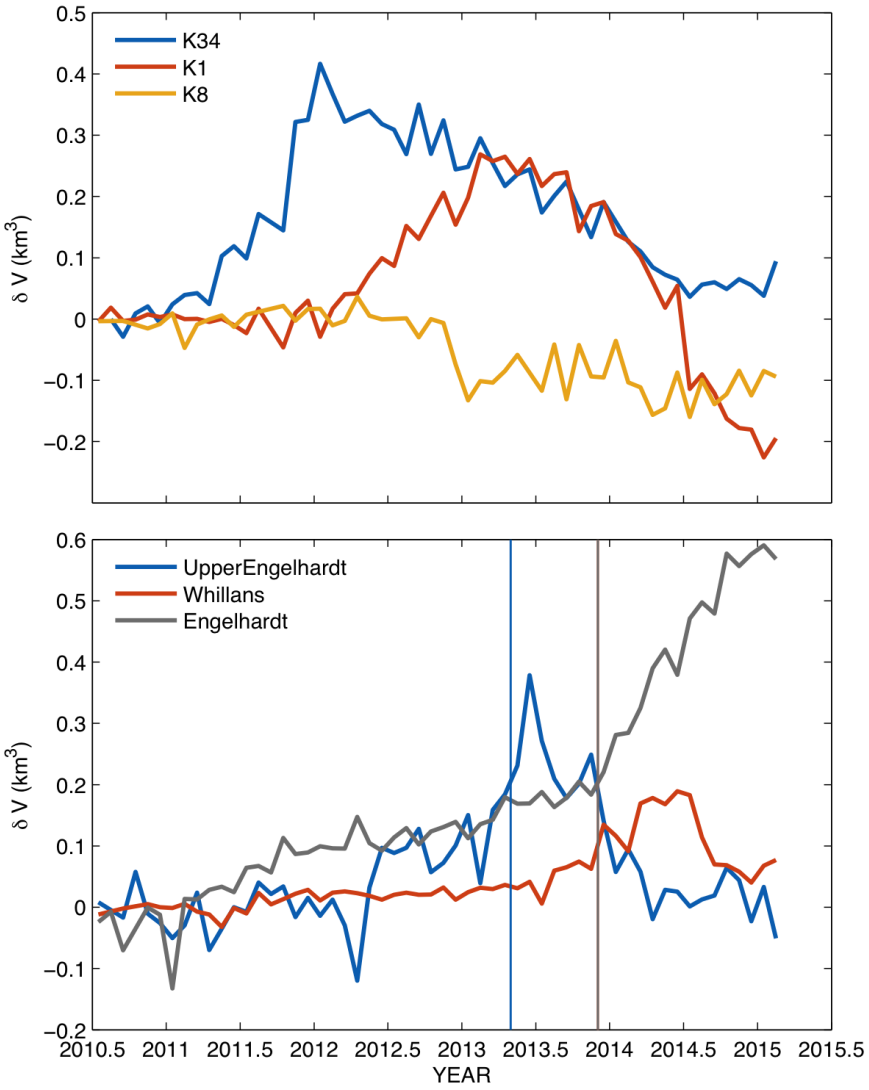

Figure 6.1. Volume changes in the lakes upstream of KIS (upper panel) and the lakes in WIS (lower panel). The vertical lines in lower panel show the start times of filling of UpperEngelhardt and Engelhardt indicating the water velocity of about 48 m/hr.

Meanwhile, sequential SGL activities were occurred at the same period in WIS (lower panel of Figure 6.1). The filling in the lakes in WIS, UpperEngelhardt and Engelhardt, may be connected with the drainage of K1, because the start times of sudden filling are similar to those of KTs and the hydrological connectivity between KIS and WIS has been suggested by a few model predictions [*Carter and Fricker*, 2012; *Goeller et al.*, 2015]. However, the gradual filling before 2013 seems to be caused by other sources such as water supplies from the upstream region of WIS. The water velocity between the UpperEngelhardt and Engelhardt is about 48 m/hr similar to those in the trunk of KIS. In order to understand the subglacial connectivity between KIS and WIS more precisely, the further research about basal topography and ice surface topography of the inland side of Siple Coast Ice Stream would be needed.

We have investigated the hydrological activities that occurred in the basal plane using the temporal surface elevation pattern on the KIS downstream. If we can estimate the next drainage activities occurring in this area in the next few years, using a wide range of observation method, including altimeter, will be able to derive improved results. In the state that the channelized subglacial water continues to exist without any freezing effect, perhaps this region is very likely to occur the periodic subglacial activities in accordance with drainage of upper trunk SGLs (e.g. Kamb 1 or Kamb 4). Also the Kamb trunk system has advantage of simplicity, which certainly interconnected in a line. In addition, in the estuary the drainage response triggered by upstream subglacial activity is very clear. Therefore, an further study in this region cannot be limited to just

examine the short periodic subglacial water activity, but also can be appropriate to design a coupled model between subglacial activity and ice dynamics.

Chapter 7. Conclusion

Using Cryosat-2 radar altimeter, we observed recent elevation changes associated with SGLs in three areas nearby Ross Ice Shelf in Antarctica. We developed a semi-automatic method to detect ice elevation changes and successfully observed time-variant ice topography due to SGLs activity in WIS and KIS while the method is limited to apply for rugged terrain such as David Glacier. In particular, it is remarkable that three additional subglacial lakes are discovered, and we also found that the vertical displacement of ice surface elevation in KIS estuary. These founding would be very important to understand ice movement and subglacial water activities in this area. On the other hand, this study suggests further efforts to resolve a few issues. It is still uncertain how the triangle-shaped elevation change near grounding line in KIS has been occurred. The drainage and refilling patterns of KTs have to be explained by an appropriate mechanism. Moreover, the WIS & KIS's vigorous subglacial activities in 2013 are possibly attributed to a common geophysical event. Longer satellite remote sensing and in-situ observations over the regions should be helpful to understand these puzzles.

References

Beem, L. H., S. M. Tulaczyk, M. A. King, M. Bougamont, H. A. Fricker, and P. Christoffersen, 2014, Variable deceleration of Whillans Ice Stream, West Antarctica, *Journal of Geophysical Research: Earth Surface*, *119*(2), 212–224, doi:10.1002/2013jf002958.

Carter, S. P., and H. A. Fricker, 2012, The supply of subglacial meltwater to the grounding line of the Siple Coast, West Antarctica, *Annals of Glaciology*, *53*(60), 267–280, doi:10.3189/2012AoG60A119.

Catania, G., T. A. Scambos, H. Conway, and C. F. Raymond, 2006, Sequential stagnation of Kamb Ice Stream, West Antarctica, *Geophysical Research Letters*, *33*(14), doi:10.1029/2006gl026430.

Engelhardt, H., and B. Kamb, 1997, Basal hydraulic system of a West Antarctic Ice Stream: Constraints from borehole observations, *Journal of Glaciology*, *43*(144), 207–230.

Flament, T., E. Berthier, and F. Remy, 2014, Cascading water underneath Wilkes land, East Antarctic ice sheet, observed using altimetry and digital elevation models, *Cryosphere*, *8*(2), 673–687, doi:10.5194/tc-8-673-2014.

Flowers, G. E., 2015, Modelling water flow under glaciers and ice sheets, *Proceedings of the Royal Society a-Mathematical Physical and Engineering Sciences*, *471*(2176), doi:ARTN 20140907 10.1098/rspa.2014.0907.

Fountain, A. G., 1992, Subglacial water flow inferred from stream measurement at South Cascade Glacier, Washington, U.S.A, *Journal of Glaciology*, *38*(128), 51–64.

Fretwell, P., H. D. Pritchard, D. G. Vaughan, J. L. Bamber, N. E. Barrand, R. Bell, C. Bianchi, R. G. Bingham, D. D. Blankenship, G. Casassa, G. Catania, D. Callens, H. Conway, A. J. Cook, H. F. J. Corr, D. Damaske, V. Damm, F. Ferraccioli, R. Forsberg, S. Fujita, Y. Gim, P. Gogineni, J. A. Griggs, R. C. A. Hindmarsh, P. Holmlund, J. W. Holt, R. W. Jacobel, A. Jenkins, W. Jokat, T. Jordan, E. C. King, J. Kohler, W. Krabill, M. Riger-Kusk, K. A. Langley, G. Leitchenkov, C. Leuschen, B. P. Luyendyk, K. Matsuoka, J. Mouginot, F. O. Nitsche, Y. Nogi, O. A. Nost, S. V. Popov, E. Rignot, D. M. Rippin, A. Rivera, J. Roberts, N. Ross, M. J. Siegert, A. M. Smith, D. Steinhage, M. Studinger, B. Sun, B. K. Tinto, B. C. Welch, D. Wilson, D. A. Young, C. Xiangbin, and A. Zirizzotti, 2013, BEDMAP2: improved ice bed, surface and thickness datasets for Antarctica, *Cryosphere*, *7*(1), 375–393, doi:10.5194/tc-7-375-2013.

Fricker, H. A., and T. Scambos, 2009, Connected subglacial lake activity on lower Mercer and Whillans Ice Streams, West Antarctica, 2003-2008, *Journal of Glaciology*, *55*(190), 303–315.

Fried, M. J., C. L. Hulbe, and M. A. Fahnestock, 2014, Grounding-line dynamics and margin lakes, *Annals of Glaciology*, *55*(66), 87–96, doi: 10.3189/2014AoG66A216.

Goeller, S., V. Helm, M. Thoma, and K. Grosfeld, 2015, Subglacial hy-

drology indicates a major shift in dynamics of the West Antarctic Ross Ice Streams within the next two centuries, *The Cryosphere Discussions*, *9*(4), 3995–4018, doi:10.5194/tcd-9-3995-2015.

Goovaert, 1997, Geostatics for natural resources evaluation, applied geophysics series, xiv +, new york, oxford, 496p.

Gray, L., 2005, Evidence for subglacial water transport in the West Antarctic ice sheet through three-dimensional satellite radar interferometry, *The Cryosphere Discussions*, *32*(3), doi:10.1029/2004gl021387.

Haran, T., J. Bohlander, T. Scambos, T. Painter, and M. Fahnestok, 2014, Modis Mosiac of Antarctica 2008-2009(moa2009) image map, ['moa0125' dataset]. Boulder, Colorado USA. NSIDC: National Snow and Ice Data Center. http:/dx.doi.org/10.7265/n5kp8037. 20151101.

Helm, V., A. Humbert, and H. Miller, 2014, Elevation and elevation change of Greenland and Antarctica derived from Cryosat-2, *Cryosphere*, *8*(4), 1539–1559, doi:10.5194/tc-8-1539-2014.

Joughin, I., and S. Tulaczyk, 2002, Positive mass balance of the Ross Ice Streams, West Antarctica, *Science*, *295*(5554), 476–80, doi:10.1126/science.1066875.

Kamb, B., C. F. Raymond, W. D. Harrison, H. Engelhardt, K. A. Echelmeyer, N. Humphrey, M. M. Brugman, and T. Pfeffer, 1985, Glacier surge mechanism - 1982-1983 surge of Variegated Glacier, Alaska, *Science*, *227*(4686), 469–479, doi:DOI 10.1126/science.227.4686.469.

Le Brocq, A. M., N. Ross, J. A. Griggs, R. G. Bingham, H. F. J. Corr, F. Ferraccioli, A. Jenkins, T. A. Jordan, A. J. Payne, D. M. Rippin, and M. J. Siegert, 2013, Evidence from ice shelves for channelized meltwater flow beneath the Antarctic ice sheet, *Nature Geoscience*, *6*(11), 945–948, doi:10.1038/ngeo1977.

Ligtenberg, S. R. M., M. M. Helsen, and M. R. van den Broeke, 2011, An improved semi-empirical model for the densification of Antarctic firn, *Cryosphere*, *5*(4), 809–819, doi:10.5194/tc-5-809-2011.

McMillan, M., H. Corr, A. Shepherd, A. Ridout, S. Laxon, and R. Cullen, 2013, Three-dimensional mapping by Cryosat-2 of subglacial lake volume changes, *Geophysical Research Letters*, *40*(16), 4321–4327, doi:10.1002/grl.50689.

McMillan, M., A. Shepherd, A. Sundal, K. Briggs, A. Muir, A. Ridout, A. Hogg, and D. Wingham, 2014, Increased ice losses from Antarctica detected by Cryosat-2, *Geophysical Research Letters*, *41*(11), 3899–3905, doi:10.1002/2014gl060111.

Oswald, G. K. A., and G. d. Q. Robin, 1973, Lake beneath the Antarctic ice sheet, *Nature*, *245*, 251–254.

Retzlaff, R., and C. R. Bentley, 1993, Timing of stagnation of Ice stream C, West antarctica from short-pulse-radar studies of buried surface crevasses, *Journal of Glaciology*, *39*, 553–561.

Rignot, E., J. Mouginot, and B. Scheuchl, 2011, Ice flow of the Antarctic ice sheet, *Science*, *333*(6048), 1427–30, doi:10.1126/science.1208336.

Robin, d., C. W. M. Swithinbank, and B. M. E. Smith, 1970, Radio echo exploration of the Antarctic ice sheet, *International Association of Scientific Hydrology Publication*, *86*, 97–115.

Schwanghart, W., and N. J. Kuhn, 2010, Topotoolbox: A set of matlab functions for topographic analysis, *Environmental Modelling & Software*, *25*(6), 770–781, doi:10.1016/j.envsoft.2009.12.002.

Siegert, M. J., 2005, Lakes beneath the ice sheet: The occurrence, analysis, and future exploration of lake Vostok and other Antarctic subglacial lakes, *Annual Review of Earth and Planetary Sciences*, *33*(1), 215–245, doi:DOI 10.1146/annurev.earth.33.092203.122725.

Siegert, M. J., and J. K. Ridley, 1998, An analysis of the ice-sheet surface and subsurface topography above the Vostok station subglacial lake, Central East Antarctica, *Journal of Geophysical Research-Solid Earth*, *103*(B5), 10,195–10,207, doi:Doi 10.1029/98jb00390.

Siegert, M. J., N. Ross, H. Corr, B. Smith, T. Jordan, R. G. Bingham, F. Ferraccioli, D. M. Rippin, and A. Le Brocq, 2014, Boundary conditions of an active West Antarctic subglacial lake: implications for storage of water beneath the ice sheet, *Cryosphere*, *8*(1), 15–24, doi:10.5194/tc-8-15-2014.

Siegfried, M. R., H. A. Fricker, M. Roberts, T. A. Scambos, and S. Tulaczyk, 2014, A decade of West Antarctic subglacial lake interactions from combined ICESat and Cryosat-2 altimetry, *Geophysical Research Letters*, *41*(3), 891–898, doi:10.1002/2013gl058616.

Smith, B. E., H. A. Fricker, I. R. Joughin, and S. Tulaczyk, 2009, An inventory of active subglacial lakes in Antarctica detected by ICESat (2003-2008), *Journal of Glaciology*, *55*(192), 573–595.

Stone, D. B., and G. K. C. Clarke, 1996, In situ measurements of basal water quality and pressure as an indicator of the character of subglacial drainage systems, *Hydrological Processes*, *10*(4), 615–628, doi: 10.1002/(SICI)1099-1085(199604)10:4¡615::AID-HYP395¿3.0.CO;2-M.

Wang, F., J. L. Bamber, and X. Cheng, 2015, Accuracy and performance of Cryosat-2 sarin mode data over Antarctica, *Ieee Geoscience and Remote Sensing Letters*, *12*(7), 1516–1520, doi: 10.1109/LGRS.2015.2411434.

Wingham, D. J., C. R. Francis, S. Baker, C. Bouzinac, D. Brockley, R. Cullen, P. de Chateau-Thierry, S. W. Laxon, U. Mallow, C. Mavrocordatos, L. Phalippau, G. Ratier, L. Rey, F. Rostan, P. Viau, and D. W. Vallis, 2006, Cryosat: A mission to determine the fluctuations in earth's land and marine ice fields, *Natural Hazards and Oceanographic Processes from Satellite Data*, *37*(4), 841–871, doi: 10.1016/j.asr.2005.07.027.

Wouters, B., A. Martin-Espanol, V. Helm, T. Flament, J. M. van Wessem, S. R. Ligtenberg, M. R. van den Broeke, and J. L. Bamber, 2015, Glacier mass loss. dynamic thinning of glaciers on the Southern Antarctic Peninsula, *Science*, *348*(6237), 899–903, doi:10.1126/science.aaa5727.

Wright, A., and M. Siegert, 2012, A fourth inventory of Antarc-

tic subglacial lakes, *Antarctic Science*, *24*(6), 659–664, doi: 10.1017/S095410201200048x.

국문초록

Cryosat-2 위성 고도계를 이용한 남극 빙저호 연구

서울대학교 대학원
과학교육과 지구과학 전공
김 병 훈

빙저호 수위의 변동은 빙저호 상부 표면에 수직 변위를 유발하기 때문에 인공위성 고도계를 이용한 표면 고도 변화 관측을 통하여 많은 빙저호가 발견되어 왔다. 이 논문에서는 유럽항공우주국에서 발사된 Cyrosat-2라는 최신의 위성 고도계 자료를 활용하여 남극 지역의 빙저호를 연구하였다. 그 결과, 기존에 알려진 빙저호들을 더 높은 해상도로 관측할 수 있었을 뿐더러, 기존에 밝혀지지 않은 빙저호들까지 새롭게 찾아낼 수 있었다. 특히 Kamb 빙류와 Whillans 빙류라고 불리우는 곳은 이 논문의 주요 연구 지역이다. 이 지역에서는 세 개의 새로운 빙저호가 발견되었는데, 이는 각각 Kamb Trunk 1,2 그리고 Upper Engelhardt라고 명명되었다. 이 빙저호들은 해당 지역의 수문학적 환경에 대해 우리에게 알려주는 바가 많다. 첫째로, Kamb Trunk 1과 Kamb Trunk 2 빙저호의 경우, 그 활동 양상을 통해 해당 지역의 얼음과 기반암 사이의 경계면에서 액체상태의 물이 어떤 유형으로 흐르고 있는지 유추할 수 있다. 둘째로, Kamb 빙류 유역의 하구 유역에서 삼각형 모양의 특이한 수직 변위가 발견되었다. 이 현상의 발생시기는 상류의 빙저 활동 시기와 일치하는데, 이를 통해 상류의 물 공급이 하류의 얼음 두께 변화에 어떻

게 영향을 미칠 수 있는지를 알아낼 수 있다. 마지막으로, UpperEngelhardt 빙저호의 발견 또한 해당 지역의 빙저 수문학적 지리를 밝혀내는 데에 매우 중요한 단서가 된다. 빙저호의 거동으로부터 유추한 빙저수 흐름의 경로는 최근의 여러 연구들에서 제시하는 모의실험 결과들과 잘 부합되고 있다.

주요어: 빙저호, Cryosat-2, 위성 레이더 고도계, 남극

학 번: 2014-20974